



Activated Charcoal/Alginate Nanocomposite Beads for Efficient Adsorption of the Cationic Dye Methylene Blue: Kinetics and Equilibrium

Ragab E Abouzeid¹ · Ramzi Khiari^{2,3,4} · Korany A. Ali⁵

Received: 24 September 2022 / Accepted: 2 December 2022 / Published online: 17 December 2022
© The Tunisian Chemical Society and Springer Nature Switzerland AG 2022

Abstract

Novel adsorbent composite beads based on sodium alginate/Activated charcoal (SA/AC) were prepared. The beads were characterized using a variety of instruments, including a Fourier transform infrared spectrometer (FTIR), and scanning electron microscope (SEM). The adsorption capacity of the beads was investigated using batch adsorption studies. This study investigated the influence of several parameters, including the initial pH of the MB solution, the contact time, the initial concentration of the MB, and the temperature of the MB solution. Methylene blue (MB) was effectively adsorbing on sodium alginate/activated charcoal beads after 60 min. The adsorption process was fitted with a pseudo-second-order kinetic model, yielding maximum adsorption capacities of 555 mg/g in mildly alkaline solutions SA/AC beads were development to be capable of regenerating the MB up to four times without compromising their adsorption efficiency. The SA/AC beads were found to be excellent adsorbents for organic contaminants in wastewater in this investigation.

Keywords Sodium alginate · Charcoal nanoparticle · Methylene blue · Wastewater

1 Introduction

Pollutants can cause eye sickness, cyanosis, vomiting, shortness of breath, burns, and other health problems. Some of the industries that make these pollutants are paper, printing, leather, textiles, electroplating, and cosmetics [1–4]. They have a huge impact on human health and the environment because the majority of them are toxic and non-degradable.

As a result, it's critical to get rid of these harmful chemicals from the water supply. Adsorption technology, the easiest and most cost-effective treatment method among chemical, physical, and biological treatments, is widely used [5]. A common type of direct dye is anionic and water-soluble, making it easy to apply and cost-effective in the textile industry. Viscose dyeing, silk and silk printing, leather dyeing, the production of organic pigment sediment color, etc. all employ methylene blue, a commercial dye [6–9]. As a result, scientists are focusing their efforts on developing new technologies for removing MB from contaminated water. To date, several strategies have been used to extract or degrade MB from contaminated water systems, including biological, physical, and chemical approaches [1, 10, 11]. Adsorption, coagulation, biological processes, membrane separation, ion exchange methods, and flocculation techniques are some of the ways used to remove harmful compounds from wastewater. Other approaches include photocatalytic degradation and electrochemical procedures that are used for these purposes [12–16]. Separating hazardous compounds from industrial effluents can be accomplished using any of these methods. However, new solutions are constantly being looked at because current procedures are either ineffective or produce harmful waste. This method of dye separation has

✉ Ragab E Abouzeid
r_abouzeid2002@yahoo.com

¹ Cellulose and Paper Department, National Research Centre, Giza 12622, Egypt

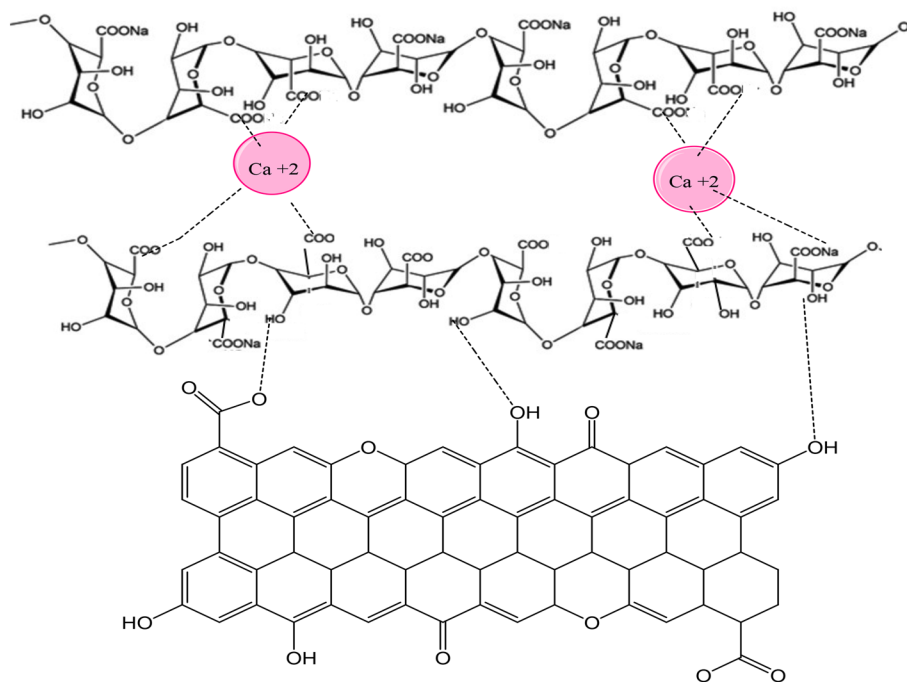
² Faculty of Sciences of Monastir, Laboratory of Environmental Chemistry and Clean Process (LCE2P-LR21ES04), University of Monastir, 5019 Monastir, Tunisia

³ Department of Textile, Higher Institute of Technological Studies of Ksar Hellal, Ksar Hellal, Tunisia

⁴ Univ. Grenoble Alpes, CNRS, Grenoble INP, LGP2, F-38000 Grenoble, France

⁵ Applied Organic Chemistry Department, Center of Excellence for Advanced Science, National Research Centre, Giza 12622, Egypt

Scheme 1 Schematic presentation of alginate activated charcoal structure



become popular because of its superior performance. Adsorbents are readily available, the operation is simple, and reusability and regeneration are cost-effective. Therefore, it is widely utilized around the world. Due to its pilot-scale use, the adsorption approach can be used to offer exact feedback for industrial-scale operations [17–19]. A carbon nanoparticle (CNP) is a form of carbon that is non-graphite and can be produced by activating carbon obtained from agricultural wastes, such as coconut shells, bamboo, wood chips, or sawdust. Two steps are involved in the activation process. The raw material is first charred, then activated chemically, thermally, or with steam to drive the highly porous material [20]. The high porosity, huge surface area, and thermal stability of CNP improve its adsorption efficiency by making it a flexible adsorbent. That led to the usefulness of CNP for wastewater treatment. Its high production costs make it prohibitively expensive, which leads to the limits of its use most of the time. As a result, companies are scrambling to find raw materials for making CNP that are less expensive, more readily available, and more efficient [21–23]. Various doping approaches, such as the addition of additional functional groups and cross-linking, have been used to improve the efficiency of alginate-beads for MB adsorption. The use of lignocellulosic biomass is suggested as an alternative carbon precursor because it is abundant, renewable, and low in cost [1, 24, 25]. The surfactant-impregnated AC-alginate beads ability to remove MB has not been studied. In light of the above [26, 27]. From these findings and in continuation of our efforts to produce several matrices of biodegradable composites for industrial and environmental applications [1, 28–31], we have constructed a composite from alginate and

CNP in the form of microsphere beads with a highly porous structure for efficient removal of methylene blue as an example of an industrial dye.

2 Experimental

2.1 Materials

All chemicals such as calcium chloride (CaCl_2 , 98%), MB Sodium alginate (98%), sodium hydroxide (NaOH , 99%), activated charcoal and hydrochloric acid (37%) having molecular were provided by Sigma Aldrich. As well as sodium hydroxide, hydrochloric acid, and activated charcoal were purchased from Merck, Germany.

2.2 Preparation of Alginate/Activated Charcoal Nanocomposite Beads

Sodium alginate and charcoal nanoparticle composite beads (SA/AC) were prepared by dissolving 2 g sodium alginate in 100 mL distilled water for 3 h. To remove any remaining gas bubbles, the resultant solution was degassed by sonication for 2 h. 0.2 g of active charcoal was added to the alginate solution at room temperature and stirred for 3 h. Using the NRC-5 Pro microencapsulation device (developed and built by our group), we made SA/AC composite beads by dropping an alginate Active charcoal solution into a magnetically stirred 3% (w/v) CaCl_2 solution. The proposed chemical structure of SA/AC is illustrated in Scheme 1.

2.3 Characterizations

Shimadzu FT-IR Spectrophotometer (8007S) spectra were measured from 500 to 4000 cm^{-1} at 4 cm^{-1} resolution. SEM was carried out using JEOL JEM-2100 electron microscope equipped with 100 \times magnification and 120 kV acceleration voltage was used to obtain an image of the SA and AC/SA beads. Thermal analysis (STA6000, Perkinelmer) was performed at 10 $^{\circ}\text{C}/\text{min}$.

2.4 Adsorption Studies

A stock solution of MB with a concentration of 2000 ppm was diluted with water to produce a series of aqueous solutions with varying concentrations. The following measures were taken in general: SA/AC nanocomposite beads are prepared in MB solution using appropriate starting concentrations and time intervals. A spectrophotometer (UNICO UV-2000) was used to measure the aliquots at maximum absorbance (668 nm). It is possible to conduct batch adsorptions by adsorbing to SA/AC composite beads regularly, in a variety of pH solutions, and at regular intervals. The following equation was used to determine the amount of MB dye adsorbed on SA/AC composite beads at the adsorption equilibrium (in mg/g).

$$q_e = ((C_o - C_e)V)/W \quad (1)$$

Concentrations of dye at initial and equilibrium (C_o and C_e respectively) in SA/AC nanocomposite bead solution (mg/L), dye solution volume in L (V), and nanocomposite weight (W) (g).

In order to investigate the recyclability of beads, we mixed 10 mg with 20 mL of MB solution using a batch concentration of 100 mg/L and a pH of 8. The beads were then agitated with 0.5 M sodium chloride in $\text{C}_2\text{H}_5\text{OH}$ (50:50 v/v) solution as an adsorbing reagent. The beads were utilised four times, with Eq. (2).

$$\text{Desorption} = \frac{\text{Mass Desorbed}}{\text{Mass Adsorbed}} \quad (2)$$

3 Results and Discussion

3.1 Adsorbent Characterization

3.1.1 SEM

To characterize the surface structure of beads produced, scanning electron microscopy (SEM) was used. At various magnifications, SEM images indicated a high degree of porosity and a number of voids in the morphology. As illustrated in Fig. 1, the surface of the beads was extremely porous, providing additional active sites for MB adsorption. Because the porous structure of alginate active charcoal provides high surface area of 650 m^2/g for MB adsorption, its capacity to absorb MB molecules has improved.

3.1.2 FTIR Spectra

The FTIR spectra for SA, and SA/AC beads before and after MB adsorption are shown in Fig. 2. The peak at 3400 cm^{-1} corresponds to the hydroxyl group ($-\text{OH}$ group). The peak shifts to 3300 cm^{-1} after MB adsorption which represents the H-bonding interaction between SA/AC beads and MB. Also, significant peaks were appeared in the spectra after MB adsorption such as at 1314 cm^{-1} (C–N stretching), 1407 cm^{-1} (N–H), and 1592 cm^{-1} (C=N of aromatic ring).

3.1.3 TGA

In Fig. 3, the thermogravimetric analysis (TGA) and its derivatives are shown for SA and SA/AC beads with a temperature range of 25 to 700 $^{\circ}\text{C}$ and a heating rate of 10 $^{\circ}\text{C}/\text{min}$. Weight loss between 50 and 200 $^{\circ}\text{C}$ is attributed to moisture content. The degradation of SA and SA/AC

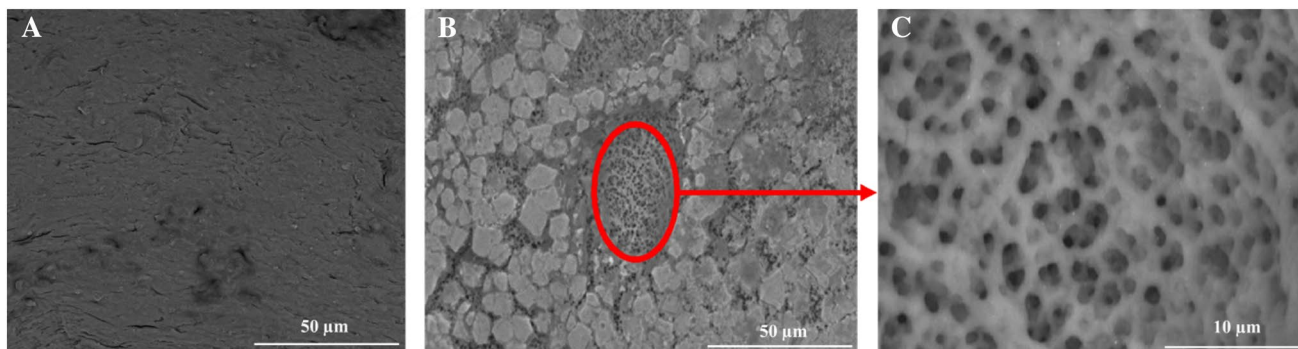


Fig. 1 SEM images of (A) sodium alginate and (B, C) sodium alginate/activated nanocomposite with different magnifications

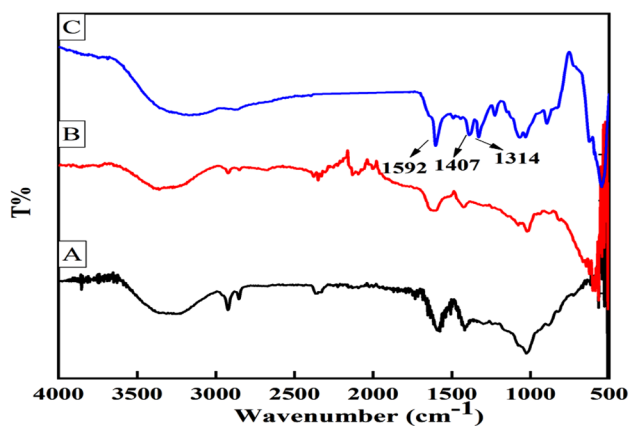


Fig. 2 FTIR analysis of (A) SA, (B) SA/AC and (C) SA/AC after dye adsorption

beads above 200 °C is caused by the thermal degradation of sodium alginate, and the final weight loss is 46 and 49%, respectively. It seems that there is no significant difference in the thermal stability with the presence of AC.

3.2 Application of the Alginate/Activated Charcoal Nanocomposite for Dye Adsorption

3.2.1 Effect of pH on the Adsorption

An adsorbent's and an adsorbate's chemical characteristics are greatly influenced by the pH of the solution in the adsorption process. A range of pH values were assessed in the current study for the adsorption of the MB dye, as shown in Fig. 4. Variation in pH can result in the ionization of the MB molecule, which then interacts with the adsorbent's surface. The MB (cationic dye) has a positive charge and

interacts strongly with negatively charged surfaces. The adsorption capacity increased with pH, reaching 94 mg/g at neutral pH. Thus, pH influences adsorption behavior affecting the adsorbent's surface quality and dye ionization. In acidic pH ranges, free protons compete with MB molecules for surface adherence. Conversely, an increase in the hydroxyl group, which might give the beads' surface a negative charge, increases the basic area's adsorption capability. This hydroxide ion increases the bead-MB molecule contact. Because pH 8 had the best MB dye adsorption capacity on the beads that were made, it was chosen as the best pH.

3.2.2 Contact Time and Adsorption Kinetics

Figure 5 shows MB dye adsorption capacity of alginate/active charcoal based on contact time. The figure shows that MB adsorption increases from 10 to 180 min of contact time. The results showed that removing MB from beads in 10–60 min was fast. Synthesized beads have more active centers on their surface, which become saturated when dye molecules adsorb. This quick increase suggested significant electrostatic force causing rapid MB cation transport towards the surface of beads. In around 120 min, the MB adsorption reached equilibrium (94 mg/g).

Different kinetic models, such as the Pseudo first and Pseudo second models, were used to determine the adsorption appliance. The linear equation for the Pseudo first kinetic model is as follows:

$$\log(q_e - q_t) = \log(q_e) - \frac{K_1}{2.303}t \quad (3)$$

Because the values of $\log(q_e - q_t)$ and t have a direct relationship, A linear plot's intercept and slope can be used to

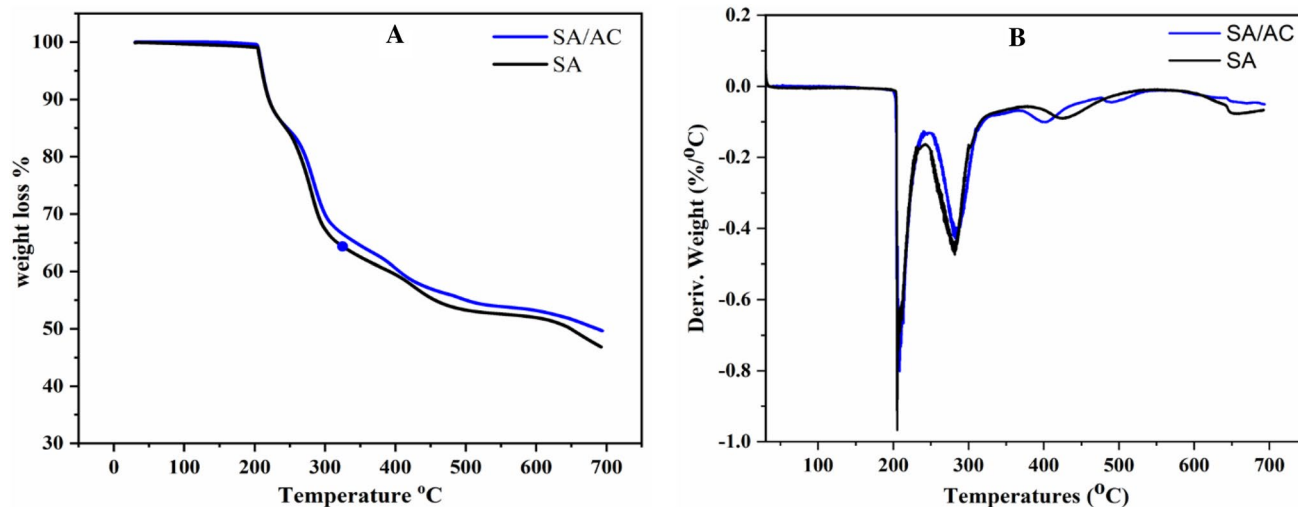


Fig. 3 (A) TGA and (B) DTG analysis of SA and SA/AC beads

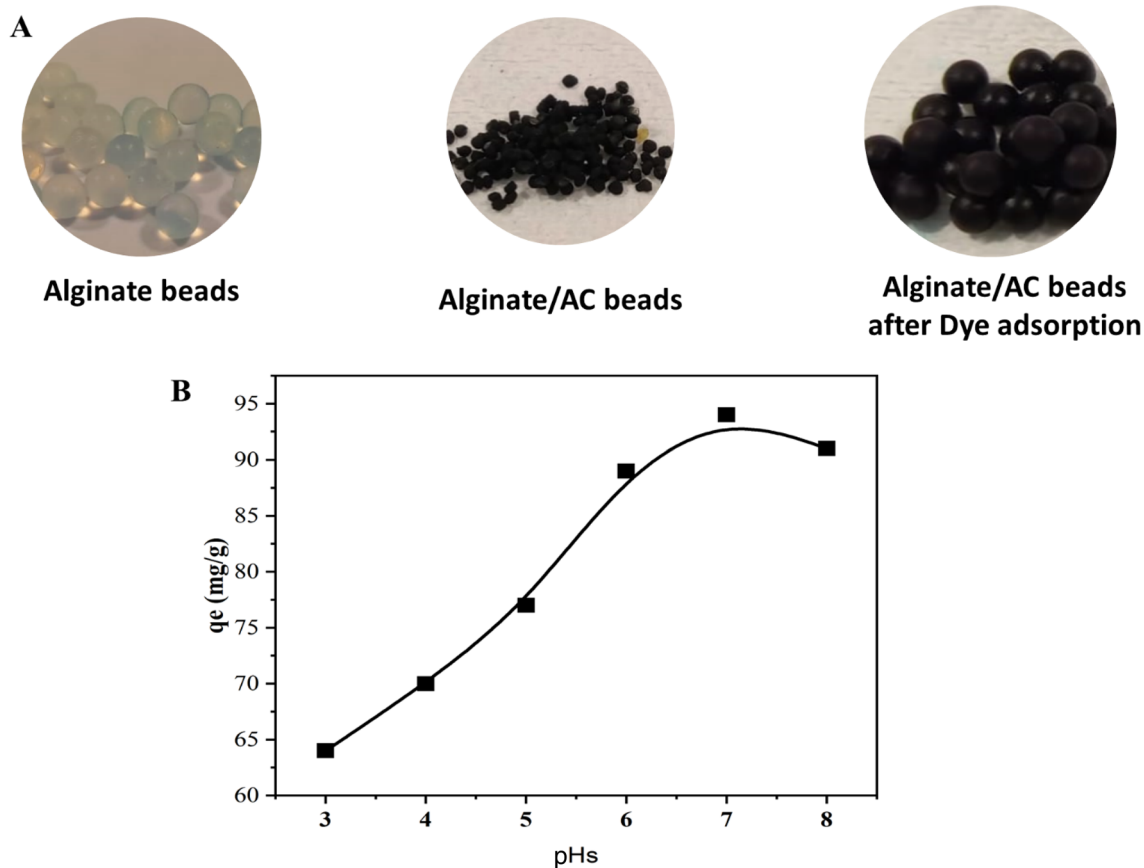


Fig. 4 **A** Picture of alginate/AC before and after dye adsorption. **B** Effect of pH on the adsorption capacities of SA/AC for MB dye. Dyes at a concentration of 100 mg/L; samples at a concentration of 0.05 g/50 mL for 120 min

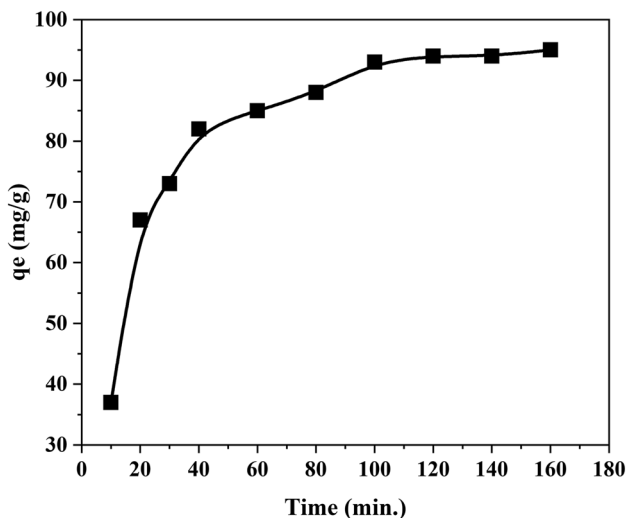


Fig. 5 Effect of contact time on MB adsorption on SA/AC beads

calculate K_1 and q_e . The R-squared value and the expected q_e value are typically used to choose the better fit (Fig. 6).

K_2 is the equilibrium rate constant for the pseudo-second kinetic model, q_e is the quantity of MB loaded on beads at equilibrium, and q_t is the amount of MB loaded on beads at any time t . The kinetics of pseudo-second are linear.

$$\frac{t}{q_t} = \frac{t}{q_e} + \frac{1}{K_2 q_e^2} \tag{4}$$

q_t (mg/g) is adsorption time, q_e (mg/g) is equilibrium adsorption, k_1 (min^{-1}) and k_2 ($\text{g mg}^{-1} \text{min}^{-1}$) are pseudo first and second model rate constants respectively.

We used pseudo first and second kinetics to analyse the experimental data for MB uptake by manufactured beads. Figure 5 shows simulated charts for the Pseudo first and second models (a, b). Also, Table 1 displays the experimentally determined MB uptake factors by alginate/AC. Compared to the pseudo first model, the pseudo second

model yields a better regression coefficient for MB. The estimated adsorption capability ($q_{cal} = 204 \text{ mg/g}$) is close to the experimentally obtained adsorption capacity ($q_{exp} = 194 \text{ mg/g}$), demonstrating that the second models kinetic accurately captures MB absorption by beads. Adsorption of MB on synthesised beads appears to be dominated through chemisorption.

3.2.3 Adsorption Isotherms

Studies of adsorption isotherms are typically used to illustrate how dye molecules diffuse across the interfaces between solids and liquids. In this study, the adsorption isotherms of nanocomposite have been calculated at various initial levels of MB concentration after reaching saturation at ambient conditions. It has been found that the Langmuir isotherm provides accurate data on homogenous adsorption and predicts the formation of monolayers on surfaces. Freundlich isotherms describe heterogeneous and multilayer surfaces. Isotherm models by Langmuir and Freundlich (Eqs. 5 and 6) are as follows:

$$\frac{C_e}{q_e} = \frac{1}{K_s q_{max}} + \frac{C_e}{q_{max}} \quad (5)$$

MB adsorbed by nanocomposites is q_e (mg/g), dye equilibrium concentration is C_e (mg/l), maximum MB is q_{max} (mg/g), and Langmuir constant is K_s (mg/l).

The Freundlich equation is given by:

$$\log q_e = \frac{1}{n} \log C_e + \log P \quad (6)$$

In this equation, P refers to adsorption capacity (mg/g) and n is a constant that represents adsorption intensity (dimensionless).

According to Table 2, these isotherm adsorption factors are reported for isotherm models. Langmuir isotherms of MB dye molecules adsorbed on a prepared nanocomposite showed a higher correlation coefficient (R^2). The high correlation coefficient indicated in the Langmuir isotherm indicates that identical adsorption sites are directly connected to the adsorbed MB-shaped monolayer. Adsorption efficiency according to the

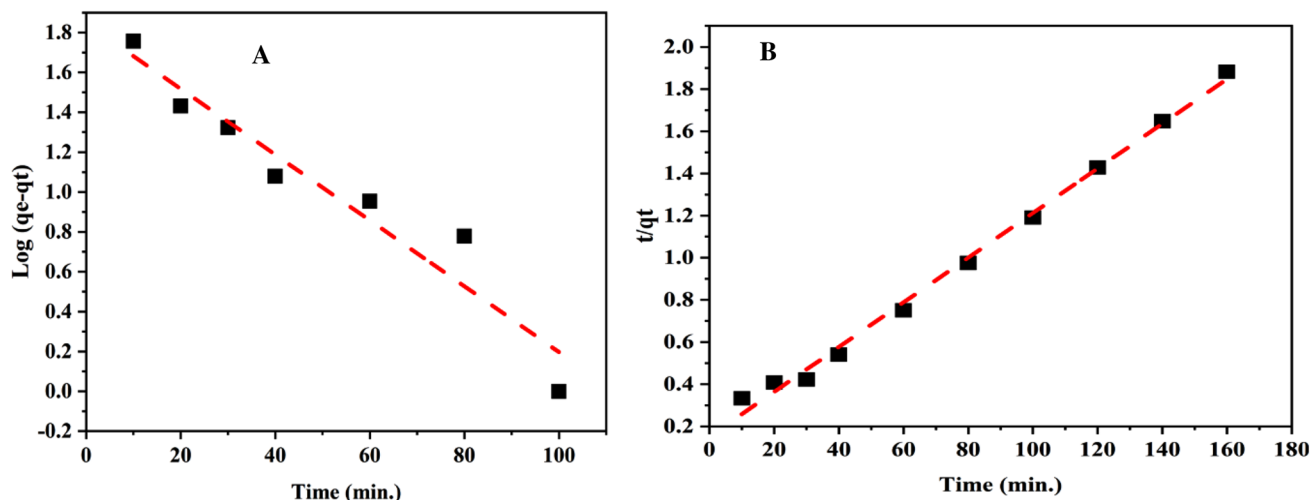


Fig. 6 Kinetic models for MB adsorption on SA/AC beads. **a** pseudo first and **b** pseudo second order

Table 1 Kinetic parameters of SA/AC nanocomposites adsorbing MB

	Pseudo first order parameters				Pseudo second order parameters		
	$q_{e\text{-exp}}$ (mg/g)	$q_{e\text{-cal}}$ (mg/g)	K_1 (min^{-1})	R^2	$q_{e\text{-cal}}$ (mg/g)	K_2 ($\text{g}(\text{mg min})^{-1}$)	R^2
SA/AC	94	71	0.037	0.92	94.5	7.35×10^{-4}	0.995

Table 2 Parameters for MB adsorption by SA/Activated charcoal nanocomposites according to different equilibrium models

	Langmuir isotherm parameters			Freundlich isotherm parameters		
	K_s (mg/L)	q_m (mg/g)	R^2	P (mg/g)	n	R^2
SA/AC	0.014	555	0.982	18.8	17.86	0.856

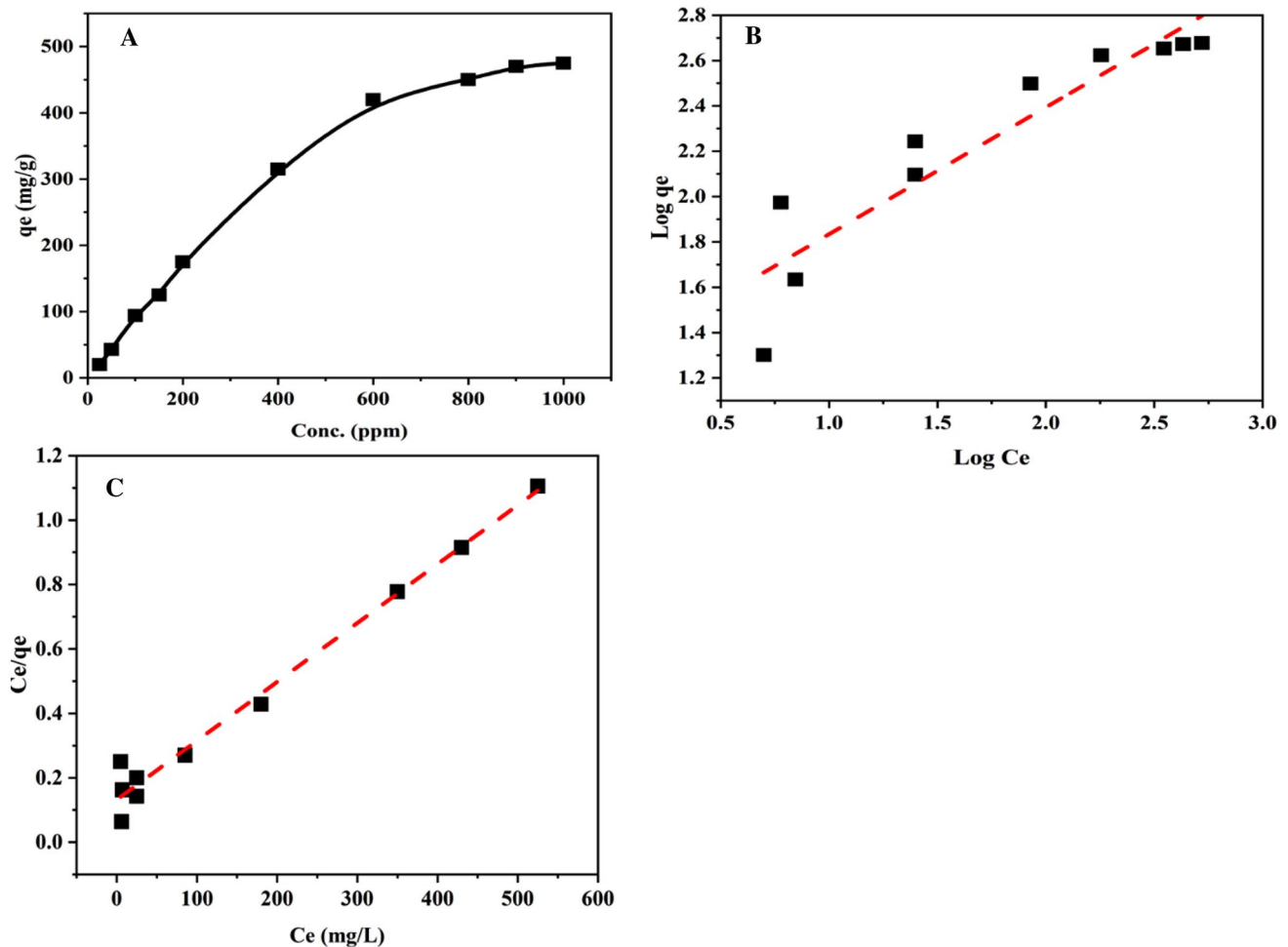


Fig. 7 MB adsorption based on (a) concentration (non-linear fitting), (b) Langmuir model (linear fitting), and (c) Freundlich model (linear fitting)

Langmuir isotherm was 555 mg/g. Figure 7 displays the results of the study for varying concentrations from 25 to 1000 mg/L. An increase in MB concentration promotes the force that moves from the solid phase to the aqueous phase, resulting in an increase in MB adsorption to the active sites on the nanocomposite. Table 2 parameters for MB adsorption by SA/Activated charcoal nanocomposites according to different equilibrium models.

3.2.4 Effect of Temperature and Thermodynamic Parameters

The temperature also affects the adsorption process. Figure 8 and Table 3 show the results of the study of the variation of the MB's adsorption capacity on A SA/AC as a function of temperature. Results show that the temperature variation

influences slightly the adsorption capacity of MB dye on SA/AC, so, the adsorption is endothermic.

Studying temperature effects on MB adsorption on SA/AC, the thermodynamic parameters including ΔH° (enthalpy), ΔS° (entropy) and ΔG° (Gibbs free energy) were evaluated. Based on Van't Hof (Eq. 7), ΔG° was calculated.

$$\Delta G^\circ = -RT \ln K_c \quad (7)$$

$$K_c = \frac{q_e}{C_e} \quad (8)$$

$$\ln K_c = \frac{\Delta S^\circ}{R} - \frac{\Delta H^\circ}{RT} \quad (9)$$

K_c is the distribution coefficient constant; R is the general gas constant ($8.314 \text{ J mol}^{-1} \text{ K}^{-1}$) and T is the absolute

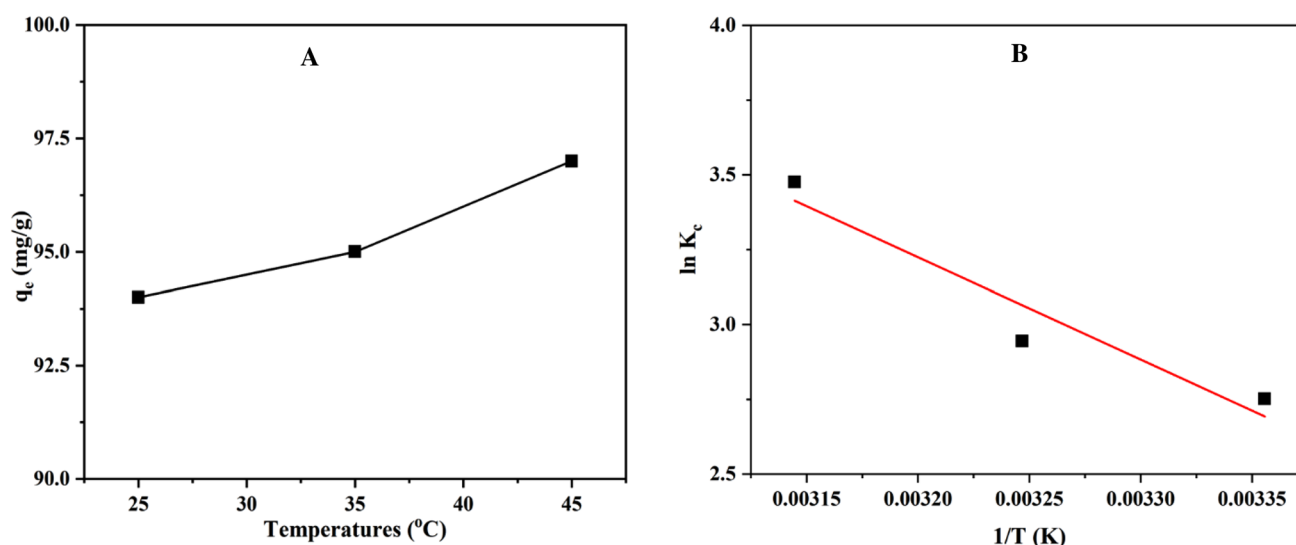


Fig. 8 (A) Effect of temperature on the adsorption capacity of MB on SA/AC, (B) Van't Hoff plot of $\ln K_c$ vs. $1/T$

Table 3 Values of thermodynamic parameters for the removal of MB on SA/AC

Sample	ΔH° (kJ mol ⁻¹)	ΔS° J mol ⁻¹ /K	ΔG° (kJ mol ⁻¹)		
			298 K	308 K	318 K
MB	28.38	116.39	-22.87	-24.48	-28.90

temperature (Kelvin). ΔH° and ΔS° values were obtained by plotting $\ln K_c$ vs $1/T$ and calculating their slopes and intercepts (Table 4).

3.3 Desorption Study

The reuse of adsorbent materials is important for industry. In Fig. 9, the results of four repeated adsorption and desorption

cycles were shown for SA/AC. With regenerated nanocomposites, after four regeneration cycles, both samples had a slightly lower adsorption capacity, 93 instead of 98. Overall, regenerated SA/AC is an effective adsorbent for removing cationic dyes.

4 Mechanism of the Adsorption

Scheme 2 show the adsorption mechanism of MB onto the surface of SA/AC adsorbent. The mechanism of the adsorption depends on the presence of different functional groups and charges on both adsorbent and adsorbates. The electrostatic interaction will occur between the cationic groups of MB with the negative groups on the surface of SA/AC groups.

Table 4 Comparison of adsorption capacities of some reported in literature and several reported AC/alginate beads

	Adsorbate (dye)	Adsorption capacity	References
Alginate-halloysite nanotube beads	MB	250 mg/g	[32]
Magnetic alginate beads	MB	0.7 mmol/g	[33]
Magnetic alginate beads	MO	0.02 mmol/g	[33]
Calcium alginate biobeads	MB	23 mg/g	[34]
GO/calcium alginate composites	MB	181.81 mg/g	[35]
Monolithic graphene oxide (GO) gels	MB	833.3 mg/g	[36]
Alginate/AC beads	MB	555 mg/g	This work

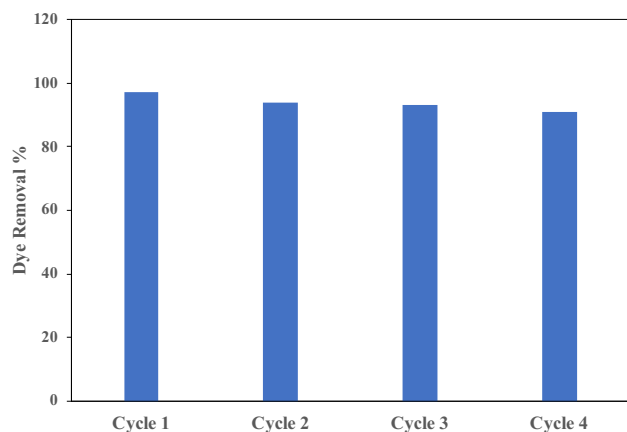
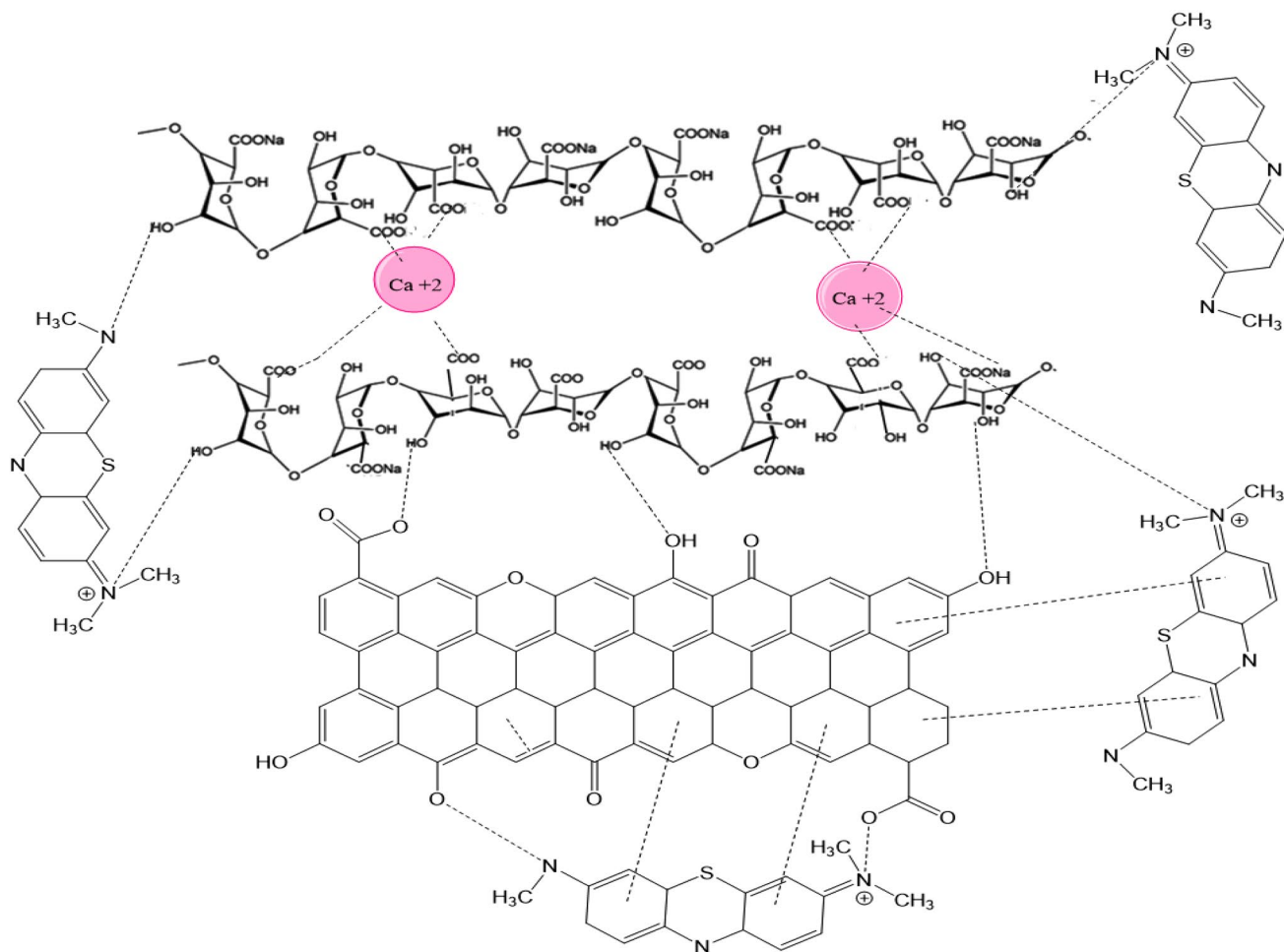


Fig. 9 Reusability of SA/AC for MB adsorption

5 Conclusions

This work proved the feasibility of producing novel low-cost and sustainable adsorbent composite materials to obtain greater MB dye removal from wastewater. Sodium alginate and charcoal nanoparticles (SA/AC beads) were successfully produced and analyzed utilizing a variety of analytical techniques. Batch adsorption testing showed a maximum capacity of 555 mg/g at pH 8. Kinetic analysis and isotherm data evaluation suggest that the Langmuir model best fits the experimental data. A dye molecule is transferred from the main solution to the external surface of the beads during the first stage, while dye intraparticle are diffused inside the pores of the beads during the second stage. Beads that have been made do not need to be thrown away after four cycles of adsorption. As a result, they have a high efficiency in removing MB, which is important for long-term and industrial-scale operations.



Scheme 2 Proposed mechanism of adsorption of SA/AC with MB dye

Acknowledgements In this work, the authors would like to express their gratitude to the National Research Centre for technical assistance.

Authors' Contributions The authors of this article and their contribution to this work are equals contributions.

Funding No funding is available.

Data Availability The research data associated with a paper is available.

Declarations

Conflict of interest The authors declare no conflict of interest. Ramzi Khiari is Guest Editor of the Special Issue "Lignocellulose at multi-scale: preparation characterization".

References

- Abouzeid RE, Khiari R, El-Wakil N, Dufresne A (2019) Current state and new trends in the use of cellulose nanomaterials for wastewater treatment. *Biomacromol* 20:573–597
- Katheresan V, Kansedo J, Lau SY (2018) Efficiency of various recent wastewater dye removal methods: A review. *J Environ Chem Eng* 6:4676–4697
- Hasanpour M, Hatami M (2020) Photocatalytic performance of aerogels for organic dyes removal from wastewaters: review study. *J Mol Liq* 309:2
- Salama A, Abou-Zeid RE, Cruz-Maya I, Guarino V (2020) Soy protein hydrolysate grafted cellulose nanofibrils with bioactive signals for bone repair and regeneration. *Carbohydr Polym*. <https://doi.org/10.1016/j.carbpol.2019.115472>
- Salama A, Abouzeid R, Leong WS et al (2021) Nanocellulose-based materials for water treatment: adsorption, photocatalytic degradation, disinfection, antifouling, and nanofiltration. *Nanomaterials* 11:2
- Salama A, Abou-Zeid RE (2021) Ionic chitosan/silica nanocomposite as efficient adsorbent for organic dyes. *Int J Biol Macromol* 188:404–410. <https://doi.org/10.1016/j.ijbiomac.2021.08.021>
- Abou-Zeid RE, Awwad NS, Nabil S et al (2019) Oxidized alginate/gelatin decorated silver nanoparticles as new nanocomposite for dye adsorption. *Int J Biol Macromol* 141:1280–1286. <https://doi.org/10.1016/j.ijbiomac.2019.09.076>
- Pires JRA, Souza VGL, Fernando AL (2019) Valorization of energy crops as a source for nanocellulose production—Current knowledge and future prospects. *Ind Crops Prod* 140:111642. <https://doi.org/10.1016/j.indcrop.2019.111642>
- El NA, Abdelwahab O, El-Sikaily A, Khaled A (2009) Removal of direct blue-86 from aqueous solution by new activated carbon developed from orange peel. *J Hazard Mater* 161:102–110. <https://doi.org/10.1016/j.jhazmat.2008.03.060>
- Gago D, Chagas R, Ferreira LM et al (2020) A novel cellulose-based polymer for efficient removal of methylene blue. *Membranes* (Basel). <https://doi.org/10.3390/membranes10010013>
- Sirajudheen P, Nikitha MR, Karthikeyan P, Meenakshi S (2020) Perceptive removal of toxic azo dyes from water using magnetic Fe₃O₄ reinforced graphene oxide–carboxymethyl cellulose recyclable composite: Adsorption investigation of parametric studies and their mechanisms. *Surfaces Interfaces*. <https://doi.org/10.1016/j.surfin.2020.100648>
- Iqbal J, Shah NS, Sayed M et al (2020) Deep eutectic solvent-mediated synthesis of ceria nanoparticles with the enhanced yield for photocatalytic degradation of flumequine under UV-C. *J Water Process Eng*. <https://doi.org/10.1016/j.jwpe.2019.101012>
- Rivera-Utrilla J, Sánchez-Polo M, Ferro-García MÁ et al (2013) Pharmaceuticals as emerging contaminants and their removal from water. A review. *Chemosphere* 93:1268–1287
- Iqbal J, Shah NS, Sayed M et al (2020) Synthesis of nitrogen-doped Ceria nanoparticles in deep eutectic solvent for the degradation of sulfamethaxazole under solar irradiation and additional antibacterial activities. *Chem Eng J*. <https://doi.org/10.1016/j.cej.2020.124869>
- Wan Ngah WS, Teong LC, Hanafiah MAKM (2011) Adsorption of dyes and heavy metal ions by chitosan composites: A review. *Carbohydr Polym* 83:1446–1456
- Li L, Iqbal J, Zhu Y et al (2020) Chitosan/Al₂O₃-HA nanocomposite beads for efficient removal of estradiol and chrysoidin from aqueous solution. *Int J Biol Macromol* 145:686–693. <https://doi.org/10.1016/j.ijbiomac.2019.12.223>
- Nasrullah A, Bhat AH, Naeem A et al (2018) High surface area mesoporous activated carbon-alginate beads for efficient removal of methylene blue. *Int J Biol Macromol* 107:1792–1799. <https://doi.org/10.1016/j.ijbiomac.2017.10.045>
- Naseer A, Jamshaid A, Hamid A et al (2019) Lignin and lignin based materials for the removal of heavy metals from waste water—An overview. *Zeitschrift fur Phys Chemie* 233:315–345
- Saber-Samandari S, Saber-Samandari S, Nezafati N, Yahya K (2014) Efficient removal of lead (II) ions and methylene blue from aqueous solution using chitosan/Fe-hydroxyapatite nanocomposite beads. *J Environ Manage* 146:481–490. <https://doi.org/10.1016/j.jenvman.2014.08.010>
- Rajabi M, Mahanpoor K, Moradi O (2017) Removal of dye molecules from aqueous solution by carbon nanotubes and carbon nanotube functional groups: Critical review. *RSC Adv* 7:47083–47090. <https://doi.org/10.1039/c7ra09377b>
- Gul Zaman H, Baloo L, Pendyala R et al (2021) Produced water treatment with conventional adsorbents and MOF as an alternative: A review. *Materials* (Basel) 14:1–29. <https://doi.org/10.3390/ma14247607>
- Abouzeid RE, Owda ME, Dacrory S (2022) Effective adsorption of cationic methylene blue dye on cellulose nanofiber/graphene oxide/silica nanocomposite: Kinetics and equilibrium. *J Appl Polym Sci* 139:e52377
- Bagheri E, Rahnema H, Hassannia MA et al (2021) Oriented polylactic acid/graphene oxide nanocomposites with high mechanical and thermal properties. *J Thermoplast Compos Mater*. <https://doi.org/10.1177/08927057211038625>
- Dardeer HM, Mahgoub MY, Abouzeid RE et al (2022) Novel pseudopolyrotaxane composite based on biopolymers: Synthesis, characterization and application in water treatment. *Environ Nanotechnol Monit Manag*. <https://doi.org/10.1016/j.enmm.2021.100639>
- Hassan E, Hassan M, Abou-zeid R et al (2017) Use of bacterial cellulose and crosslinked cellulose nanofibers membranes for removal of oil from oil-in-water emulsions. *Polymers* (Basel). <https://doi.org/10.3390/polym9090388>
- Naseer A, Hamid A, Ghauri M et al (2020) Lignin/alginate/hydroxyapatite composite beads for the efficient removal of copper and nickel ions from aqueous solutions. *Desalin Water Treat* 184:199–213. <https://doi.org/10.5004/dwt.2020.25356>
- Rajkumar M, Meenakshisundaram N, Rajendran V (2011) Development of nanocomposites based on hydroxyapatite/sodium alginate: Synthesis and characterisation. *Mater Charact* 62:469–479. <https://doi.org/10.1016/j.matchar.2011.02.008>
- Wahba MI, Hassan ME, Ali KA (2021) Chitosan-glutaraldehyde activated carrageenan-alginate beads for β -D-galactosidase covalent immobilisation. *Biocatal Biotransformation* 39:138–151. <https://doi.org/10.1080/10242422.2020.1832476>
- Ali AO, Abdalla MS, Shahein YE et al (2021) Grafted carrageenan: alginate gel beads for catalase enzyme

- covalent immobilization. *3 Biotech*. <https://doi.org/10.1007/s13205-021-02875-9>
30. Assem Y, Abou-Zeid RE, Ali KA, Kamel S (2019) Synthesis of acrylate-modified cellulose via raft polymerization and its application as efficient metal ions adsorbent. *Egypt J Chem* 62:85–96. <https://doi.org/10.21608/ejchem.2018.4005.1351>
 31. Abou-Zeid RE, Dacrory S, Ali KA, Kamel S (2018) Novel method of preparation of tricarboxylic cellulose nanofiber for efficient removal of heavy metal ions from aqueous solution. *Int J Biol Macromol* 119:207–214. <https://doi.org/10.1016/j.ijbiomac.2018.07.127>
 32. Liu L, Wan Y, Xie Y et al (2012) The removal of dye from aqueous solution using alginate-halloysite nanotube beads. *Chem Eng J* 187:210–216. <https://doi.org/10.1016/j.cej.2012.01.136>
 33. Rocher V, Bee A, Siaugue JM, Cabuil V (2010) Dye removal from aqueous solution by magnetic alginate beads crosslinked with epichlorohydrin. *J Hazard Mater* 178:434–439. <https://doi.org/10.1016/j.jhazmat.2010.01.100>
 34. Hachi M, Chergui A, Selatnia A, Cabana H (2016) Valorization of the spent biomass of *pleurotus mutilus* immobilized as calcium alginate biobeads for methylene blue biosorption. *Environ Process* 3:413–430. <https://doi.org/10.1007/s40710-016-0157-z>
 35. Li Y, Du Q, Liu T et al (2013) Methylene blue adsorption on graphene oxide/calcium alginate composites. *Carbohydr Polym* 95:501–507. <https://doi.org/10.1016/j.carbpol.2013.01.094>
 36. Ma T, Chang PR, Zheng P et al (2014) Fabrication of ultra-light graphene-based gels and their adsorption of methylene blue. *Chem Eng J* 240:595–600. <https://doi.org/10.1016/j.cej.2013.10.077>

Springer Nature or its licensor (e.g. a society or other partner) holds exclusive rights to this article under a publishing agreement with the author(s) or other rightsholder(s); author self-archiving of the accepted manuscript version of this article is solely governed by the terms of such publishing agreement and applicable law.